ELSEVIER

Contents lists available at ScienceDirect

Chemical Engineering Journal Advances

journal homepage: www.sciencedirect.com/journal/chemical-engineering-journal-advances



COSMO prediction of siloxane compounds absorption on type 3 and type 5 deep eutectic solvents

Thomas Quaid, Toufiq Reza

Department of Biomedical and Chemical Engineering and Sciences, Florida Institute of Technology, 150 West University Boulevard, Melbourne, FL 32901 United States

ARTICLE INFO

Keywords: COSMO-RS Siloxanes Deep eutectic solvents Sigma profile Excess enthalpy Absorption Thermodynamics

ABSTRACT

This study reports a Conductor-like Screening MOdel for Real Solvents (COSMO-RS) prediction for 151 type 3 (polar) and type 5 Deep Eutectic Solvents (DES, non-polar) for absorption of hexamethyldisiloxane, octamethyltrisiloxane, hexamethylcyclotrisiloxane, and octamethylcyclotetrasiloxane. Through the examination of generated sigma surfaces, sigma profiles, and sigma potentials, it was found that while the siloxane chains offer sufficiently strong hydrogen bond accepting sites, the steric hindrance of the methyl groups cause less polar solvents (type 5) to outperform the more polar ones (type 3). The thermodynamic study predicts thymol-based type 5 DES as significantly more affinitive for siloxane compounds than common conventional solvents (DEA, MEA, MDEA, menthol, and DPEG Blend) with ln γ activity coefficients reaching low as -0.64. Enthalpy of mixing study shows Vander Waals interactions dominate DES-siloxane compound interactions over hydrogen bonding by over 10x enthalpic release, clarifying discrepancy in literature on how siloxanes are solvated by DES. Thymol: Stearic acid (4:1) showed the lowest excess enthalpy of mixing at -10.4 kcal/mol. An environmental health and safety (EHS) study show the best performing DES components (camphor, capric acid, lauric acid, myristic acid, stearic acid, undecenoic acid, borneol, betaine, hexadecanoic acid, and thymol) are potentially environmentally benign and safe for operation procedures.

1. Introduction

Siloxane compounds are often originated from silicon containing consumer products such as soaps, oils, personal care products, and pharmaceuticals [1-3]. When these and other silicon containing products are collected through wastewater treatment plant and landfill facilities, they are subjected to anaerobic digestion which produces siloxane compounds [4-6]. These siloxane compounds are present in gaseous streams at concentrations of 3–24 mg/m³ in landfill gasses, and up to 127 mg/Nm³ in wastewater treatment plants [7,8]. There are more than thirty siloxane compounds identified in literature, however, four common siloxane compounds are hexamethyldisiloxane (L2), octamethyltrisiloxane (L3), hexamethylcyclotrisiloxane (D3), and octamethylcyclotetrasiloxane (D4) [9]. These siloxane compounds have been classified as persistent, bio-accumulative, and toxic [10-12]. Literature indicated that siloxane compounds could be carcinogenic, endocrine disruptors, and immunosuppressants [13-17]. During combustion of siloxane compounds containing biogas and landfill gasses, silicone deposits on the turbines or engines are often observed, which cause adverse effects to the efficiency of the energy systems [4,7,18]. As a result, siloxane compounds might need to be removed from gaseous streams through an additional upgrading process [19,20].

Several technologies that capture volatile organic compounds (VOCs) are often recommended for capturing siloxane compounds which include water scrubbing, chemical scrubbing, membrane separation, and pressure swing adsorption [21-24]. Among chemical absorbents, a handful of conventional solvents monoethanolamine (MEA), dimethanolamine (DEA), methyldiethanolamine (MDEA), polyethyleneglycol dimethyl ethers, and methanol have been utilized in the industries [25-29]. However, a new class of green solvents called deep eutectic solvents (DES) have been increasingly explored for selective separation of trace contaminants or capture of harmful chemicals like siloxane compounds [30]. DES are multicomponent solvents of hydrogen bond donor (HBD) and hydrogen bond acceptor (HBA) which form a hydrogen bond complex. DES often result in a significant melting point depression compared to the pure HBA and pure HBD [31,32]. The collection of known DES is currently divided into five types. Among them, type 3 and type 5 are considered the green due

E-mail address: treza@fit.edu (T. Reza).

https://doi.org/10.1016/j.ceja.2023.100489

^{*} Corresponding author.

to the lack of metals and are comprised of two organic hydrogen bonding paired components HBD and HBA [33]. While type 3 DES are being polar in nature, type 5 DES are comprised of HBA and HBD that form less polar complexes which offers the attribute of being hydrophobic, while maintaining the potential for environmental sustainability [34].

DES have been researched extensively regarding gasses like CO2 and sulfur containing acid gasses with high selectivity and high solubility compared to traditional solvents like MEA, DEA, etc. [30,35,36]. However, siloxane compounds have received relatively little attention when it comes to DES-based absorption. Limited to small randomly selected DES are reported in the literature but with promising results. For instance, Slupek et al. [37] analyzed type 3 DES formed with tetrapropylammonium bromide as the HBA and tetraethylene glycol as the HBD in a 1:3 ratio to absorb L2, L3, and D4 at various temperatures and times, and reported absorbance up to 5000 g/L. They determined the likely reason for good solubility was due to hydrogen bonding of the DES with the oxygen in the siloxane chains. Meanwhile, Chelstowska et al. [38] studied carvone based type 5 DES at various temperatures and times, and reported carboxylic acid HBD's showed higher absorption capabilities for siloxanes L2 and D3. Unlike Slupek et al. [37], the good solubility was proposed to be from Vander Waals interactions between DES and siloxane compounds. Villarim et al. [39] also studied type 5 DES for D4 comprised of dodecanoic, decanoic, octanoic, and nonanoic acids, at varying temperatures, and the results indicated that DES outperformed conventional solvents and Gibbs free energies at 30 °C for D4 reaching below -20 kJ/mol for the DES, where conventional solvents reached as low as -13.1 kJ/mol.

From the limited literature, it can be found that DES may be effective at absorbing siloxane compounds. However, the absorption mechanism is still not well understood. Due to the overwhelming number of HBA and HBD combinations and compositions, an efficient computational approach can be employed to gain an understanding of pertinent DES characteristics and solvation potential of specific siloxane compounds. Conductor like Solvents for Molecular Screening for Real Solvents (COSMO-RS), is an ab-initio, non-empirical software tool kit which bases thermodynamic property predictions of molecules on density functional theory (DFT) computed energy profiles. Based on the molecular structure and configuration, a charged sigma surface of a molecule is computed in COSMO-RS, which can be used to determine chemical potentials of solutes in pure and solvated forms [40]. The chemical potentials lead to computations of activity coefficient, partition co-efficient, and excess enthalpy. In the literature, COSMO-RS has been successfully used to predict volatile organic compounds (VOC) extraction by DES [41-43]. For instance, Song et al. [41] and Qin et al. [42] tested the accuracy of COSMO-RS with CO2 absorption in various DES with a result R^2 value of 0.83–0.93 with over 70 data points [41]. However, to the best of the authors knowledge, no study for absorption of four selective siloxane compounds with the scope of type 3 and type 5 DES has been reported. While some components used in this study may overlap with reported literature, the systems studied are novel for which little or no experimental analyses have been made, to the best of the authors knowledge.

The objective of this study was to determine the feasibility of type 3 and type 5 DES in absorption of siloxane compounds, and to clarify the discrepancy in literature for the energetic mechanism of absorption for siloxane compounds in DES. A total of 151 type 3 and type 5 DES was gathered from literature and were evaluated in this study to absorb four common siloxane compounds namely L2, L3, D3, and D4. Sigma surface, sigma profile, and sigma potentials were studied for the siloxane compounds to better understand their bonding characteristics. Activity coefficients were calculated for individual siloxane compounds in DES to evaluate absorptive capabilities. Excess enthalpy of mixing was computed to understand the mechanism of the absorption. Finally, the environmental health and safety (EHS) properties of the DES were examined for sustainability of the promising DES.

2. Methods

2.1. Studied siloxane compounds and DES

The four siloxane compounds studied were L2, L3, D3, and D4 which acted as representatives for the three main variations of the siloxane species: linear (L) and cyclic (D), methyl group quantity (hexyl-to-octyl) and siloxane chain length (di-to-tetra). A mixed database of 151 of known type 3 and type 5 DES were used in this study (available in table S1 along with compositions). This database was developed to include a wide range of HBA and HBD components from the type 3 and type 5 DES used in the literature. This specification was expected to allow the best chance for finding sustainable solvents and to understand the energetic nature of solubilization among DES and siloxane compounds due to the variety of energy signatures available. These absorption phenomena were studied at 25 $^{\circ}$ C and 1 atm.

2.2. COSMO-RS simulation

Thermodynamic properties of siloxane compounds, DES, and absorption were predicted through COSMO-RS. If available, molecule files for selected siloxane compounds and DES components (HBA and HBD) were gathered from the onboard database of COSMO-RS. Otherwise, molecules were imported from PubChem as SMILES files in case they were not available in the COSMO-RS onboard database. Files imported from PubChem were run in TmoleX (version 4.5.3 N) to solve for the lowest energetic geometric conformation and the sigma surface charges. All DFT calculations were performed at the basis point density functional theory b-p DFT level and Karlsruhe (Ahlrichs) def2-TZVP (default-2 Valence Triple-Zeta Polarization) basis set [44]. The chosen basis set reflects current practices and benchmarking research for similar solvents which show its robust "state of the art" alternative (TZVPD-Fine) to be insignificantly more accurate especially concerning the added computational costs. Paduszyński et al. [45] found systems for ionic liquids produced slightly more accurate results for TZVP in COSMO-RS over TZVP-Fine. The same was found by Bezold et al. [46] who studied deep eutectic solvents. HBA salts were modelled in a single .cosmo extension file. The output files from TmoleX were uploaded to COSMOConf18 for conformational analysis. The outputs of COSMOConf18 were uploaded to COSMOthermX to predict thermodynamic properties including chemical potentials (µ). Eq. (1) shows how separate functions of the sigma segments $(E_{misfib}E_{HB}, and p_s)$ are responsible for the prediction of chemical potential.

$$\mu_{s}(\sigma) = -\frac{RT}{a_{eff}} \ln \left[\int p_{s}(\sigma') e^{\left(\frac{a_{eff}}{RT} \left(\mu_{s}(\sigma') - E_{misfit}(\sigma, \sigma') - E_{HB}(\sigma, \sigma')\right)\right)} d\sigma' \right]$$
 (1)

where $\mu_s(\sigma)$ is the chemical potential as a function of sigma (σ) . σ and σ' are two interacting surface segments between two molecules prime and non-prime. a_{eff} is the effective contact area. E_{misfit} is the energetic penalty for charge and steric misfits of the segments. E_{HB} is the energy resulting from hydrogen bonding. $p_s(\sigma)$ is the distribution function. R is the ideal gas constant and T is absorption temperature. These chemical potentials are further used as a basis for COSMO-RS calculations. Further description of the COSMO-RS software fundamentals and detailed derivations (and associated assumptions) of presented equations may be found elsewhere [30,44,47,48]. Finally, the activity coefficients (γ) are calculated through Eq. (2) in COSMOthermX which represent the affinity between solvent and solute and are strong indicators of solubility [49,50].

$$\ln \gamma_s^i = \frac{\left(\mu_s^i - \mu_p^i\right)}{RT} \tag{2}$$

 $\ln \gamma_s^i$ of siloxane compound (i) in DES (s) were calculated at infinite dilution. T is the absorption temperature of the system which was kept at

Table 1

Benchmark data for siloxane D4 in DES. Values are presented for enthalpy of mixing and Gibbs free energy of solvation. Enthalpy of mixing is reported for 30 °C while Gibbs free energy of solvation is reported for three different temperatures in kJ/mol. The resulting R² value for the two datasets (calculated and experimental) equates to 0.99 showing strong qualitative relationship. The calculated values are produced by COSMO-RS.

	HBD	Composition HBA:HBD	Enthalpy of mixing (kJ/mol)	G_{solv} (kJ/mol) 30 $^{\circ}\text{C}$	G_{solv} (kJ/mol) 45 $^{\circ}C$	G_{solv} (kJ/mol) 60 $^{\circ}$ C
Calculated	Octanoic acid	1:3	-40.21	-17.44	-15.31	-13.23
Calculated	Nonanoic acid	1:3	-40.76	-17.67	-15.55	-13.47
Calculated	Decanoic acid	1:2	-41.00	-17.86	-15.74	-13.66
Experimental	Octanoic acid	1:3	-40.59	-20.47	-19.64	-18.48
Experimental	Nonanoic acid	1:3	-39.38	-20.51	-19.63	-18.64
Experimental	Decanoic acid	1:2	-40.16	-20.33	-19.57	-18.36

25 °C as similar studies report lower temperatures equate to better solubilities among DES and siloxane compounds [38,39]. Eq. (2) is used to convert $\ln \gamma_s^2$ into solubility capacity in Section 3.1 [51].

Similar to the activity coefficient, Gibbs free energy of solvation (G_{solv}) is computed as a difference in chemical potentials. As shown in Eq. (3), G_{solv} is the result from the difference of the chemical potential of the siloxane compound i in its pure phase μ_p^i and its chemical potential in the solvent phase μ_s^i at infinite dilution.

$$G_{solv} = \mu_s^i - \mu_p^i \tag{3}$$

Along with activity coefficients, another indicator of absorption is the excess enthalpy of interaction (H_{int}) [52]. Activity coefficient is limited as a study of affinity between chemicals through a measure of non-ideality, expressed through non-ideal interactions (hydrogen bonding) as confirmed by the Pearson correlation matrix in table S2. Where activity coefficient draws its importance from its relation to Hildebrand solubility, excess enthalpy of interaction (H_{int}) is a temperature derivative of Gibbs free energy, allowing for a more precise study of the contributions from each interaction type (hydrogen bond and van der Waals bond) [45,53]. These interaction types are represented through COSMOthermX parameters used to measure the total enthalpy of mixing as expressed in Eq. (4).

$$H_{int} = H_{mf} + H_{hb} + H_{vdw} \tag{4}$$

where H_{mf} is the enthalpic penalty of a misfit factor which accounts for structural, steric hindrances, and charge misalignment [54]. H_{HB} is the enthalpic contribution from hydrogen bond interactions when mixing, and H_{whw} is the Vander walls contribution [55].

Quantitative structure property relationships (QSPR) descriptors were generated from sigma potential profiles [56]. These sigma moments (M) consist of σ polynomial function ($f_i(\sigma)$) which are reported in Eq. (5) and can be used in property predictions in COSMOthermX [47]. A siloxane specific moment (M_i) is computed through Eq. (6) from the σ profile ($p(\sigma)$) of the siloxane and $f_i(\sigma)$.

$$f_i(\sigma) = \sigma^i \text{ for } i \ge 0 \tag{5}$$

$$M_i^s = \int p(\sigma) f_i(\sigma) d\sigma \tag{6}$$

The zeroth order moment (M_0^s) , where i=0) is the total surface area of the siloxane "s", the first order moment (M_1^s) , where i=1) is the total COSMO polarization charge on the surface of the given siloxane, the second moment (M_2^s) , where i=2) is a vector of total COSMO polarization energy of the molecule, the third moment (M_3^s) , where i=3) correlates to the measure of sigma profile symmetry, and the hydrogen bond donating and hydrogen bond accepting moments (M_{Hdon}^s) and M_{Hacc}^s respectively) are measurements of the siloxanes ability to act as each, respectively [54].

2.3. Absorption conditions

The absorptions were studied at 25 $^{\circ}$ C and 1 atm except for methanol that is operated below -35 $^{\circ}$ C in industry, therefore, the calculations for

methanol were run at $-40\,^{\circ}$ C and 1 atm [57,58]. The pressure was kept at 1 atm for all trials as the siloxanes have boiling points above 90 $^{\circ}$ C, thus resulting in incompressible systems at room temperature. A formal composition of Selexol was unable to be determined from literature, thus an equimolar mixture of its reported constituents (6 dimethyl ether, 8 dimethyl ether, and 9 dimethyl ether of polyethylene glycol ["DPEG Blend"]) was used [59].

2.4. VEGA environmental health and safety (EHS) modeling

The quantitative structure-activity relationship (QSAR) based software VEGA [60] was used to evaluate the EHS factors for each solvent based upon five properties: persistence, bioconcentration factor (BCF), mutagenicity, carcinogenicity, and acute toxicity. Persistence is measured in days chemical is retained in the medium. Toxicity is measured in lethal dose 50 (LD50) of units mg/kg. BCF is measured in half life nits of L/kg. Mutagenicity is measured in revertants per microgram (rev/µg). Carcinogenicity is measured in concentrations per lifespan ([C]/time). VEGA has been used extensively in literature for EHS property analysis of novel solvents [51,61,62]. VEGA relies upon a k-nearest neighbors (KNN) algorithm to predict EHS properties based upon the structure of the input molecule and its database of experimental results [63]. VEGA model was run for each of the five properties studied for camphor, capric acid, lauric acid, myristic acid, stearic acid, undecenoic acid, borneol, betaine, hexadecanoic acid, and thymol for thoroughness and cross-checking validations. The persistence models were evaluated for soil, water, and air for thoroughness. For the DES included in the EHS report, the pure components that comprise the solvent are analyzed as the DES readily dissociate in the presence of moisture and are not covalently bound. Thus, their fate in the environment would not be in the DES form but rather in the individual pure HBA and HBD forms. Furthermore, a cross validation of the results was performed through pure component safety data sheet (SDS) analysis. The National Fire Protection Association (NFPA) value rankings and the Occupational Safety and Health Administration (OSHA) Hazard Communication Standard (OHCS) categorization are used from literature for validation of VEGA results when available.

3. Results and discussion

3.1. COSMO-RS validation

Compared to other computational thermodynamic predictive methods, COSMO-RS is entirely non-empirical, requiring only the molecular structure as an input for most property predictions. This makes COSMO-RS promising for exploring novel solvents like DES. A benchmark study has been performed here to determine if reasonable accuracy exists between DES and siloxane compounds. Due to the novelty of the absorption system, limited experimental values were available thus the benchmarking is based upon a dataset of 12 data points. Table 1 presents twelve computed data points from this work comparing with twelve experimental data points derived from the work of Villarim et al. [39]. The data is comprised of Gibbs solvation energies at varying temperatures, and enthalpy of mixing at 30 °C. The enthalpic mixing values are

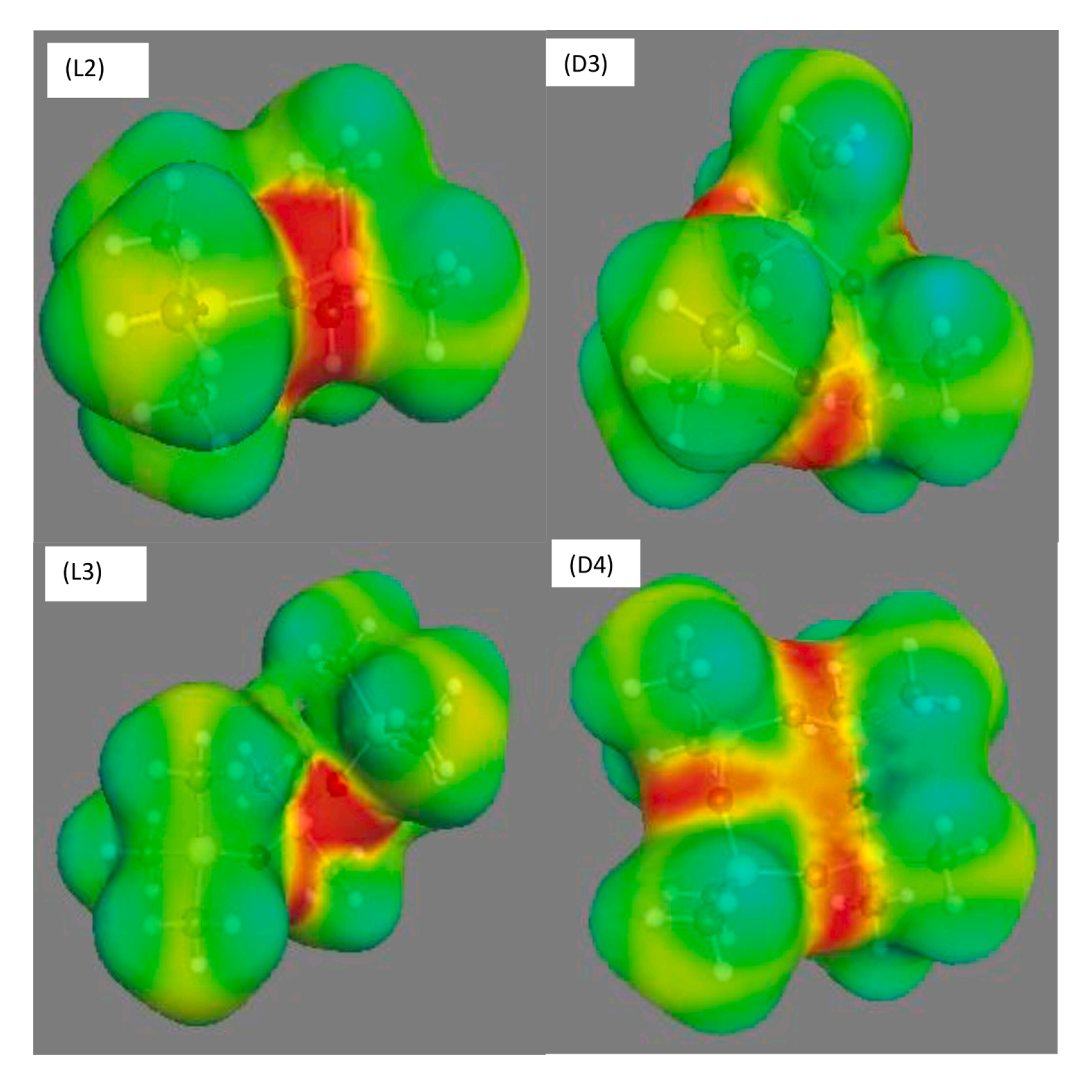


Fig. 1. Sigma surfaces of siloxane compounds as computed by TmoleX19. Charge gradient is represented by the color scale of deficient = blue, neutral = green, and dense = red. Siloxanes represented are hexamethyldisiloxane (L2), octamethyltrisiloxane (L3), hexamethylcyclotrisiloxane (D3), and octamethylcyclotetrasiloxane (D4).

very accurate with an absolute average relative deviation (AARD) of \sim 0.31%. Although it is apparent that COSMO-RS underestimates the Gibbs solvation energies with an AARD of \sim 25%.

3.2. Sigma surfaces, sigma profiles, and sigma potentials of siloxane compounds

Fig. 1 depicts the sigma surfaces of the siloxane compounds (L2, L3, D3, and D4) generated by TmoleX19. The colors represent a calculated charge gradient ranging from charge deficient to charge dense regions. The lack of significantly charge deficient regions (blue) suggests low hydrogen bond donating ability, the abundance of neutral (green) surface area indicates a strong propensity towards Vander Waals interactions, and the presence of strong charge dense regions (red) indicate hydrogen bond accepting capability. The range of the sigma values on the surfaces are from -0.011 (e/Å²) (blue) to 0.015 (e/Å²) (red). It is evident through Fig. 1 that the red regions are associated with the oxygen and blue with the methyl groups. The silicone atoms are naturally positive and contribute to the electron deficient regions (blue). Sigma surface could indicate the behavior of these molecules regarding intermolecular interactions. One such judgement is the positioning of the red sites seen in Fig. 1 suggest steric hindrance will likely produce a dampening effect to the hydrogen bond accepting potential, which is a common takeaway from sigma surfaces [64]. The difficulty for other

molecules to interact with the red regions in these sigma surfaces due to the methyl groups is quantitatively supported through computation of the QSAR determined hydrogen bond accepting moments of the siloxane molecules, as the sigma moments of two hexa-methyl siloxanes L2 and D3 (1.71, 1.83, respectively) are higher than their octa-methyl counterparts L3 and D4 at 1.25, and 1.19, respectively. These results suggest the amount of methyl groups on a siloxane compound are more determinate for hydrogen bonding capability than the linearity or siloxane chain length. Another qualitative determination may be made on the lack of sufficiently blue regions which would show affinity for hydrogen bond accepting sites on other molecules. This is confirmed quantitatively through the hydrogen bond donating moment computation which is zero for all four siloxane compounds.

Fig. 2 shows the sigma profiles of four siloxane compounds and HBA used in this study. A sigma profile offers quantitative information about the surface charge attributes and distributions and can be considered a fingerprint of the molecule [65]. The x-axis is the associated surface charge in (e/Ų), the y-axis is the frequency at which this charge segment can be found on the molecules surface or the amount of the respective color from sigma surfaces. Integration of these curves result in the total sigma surface area for each molecule present. Area between the range of $-0.079~{\rm e/Å}^2$ and $0.079~{\rm e/Å}^2$ is relevant for Vander Waals interactions. Area outside of this central region is pertinent to hydrogen bonding and ionic interactions. As no ionic interactions are expected

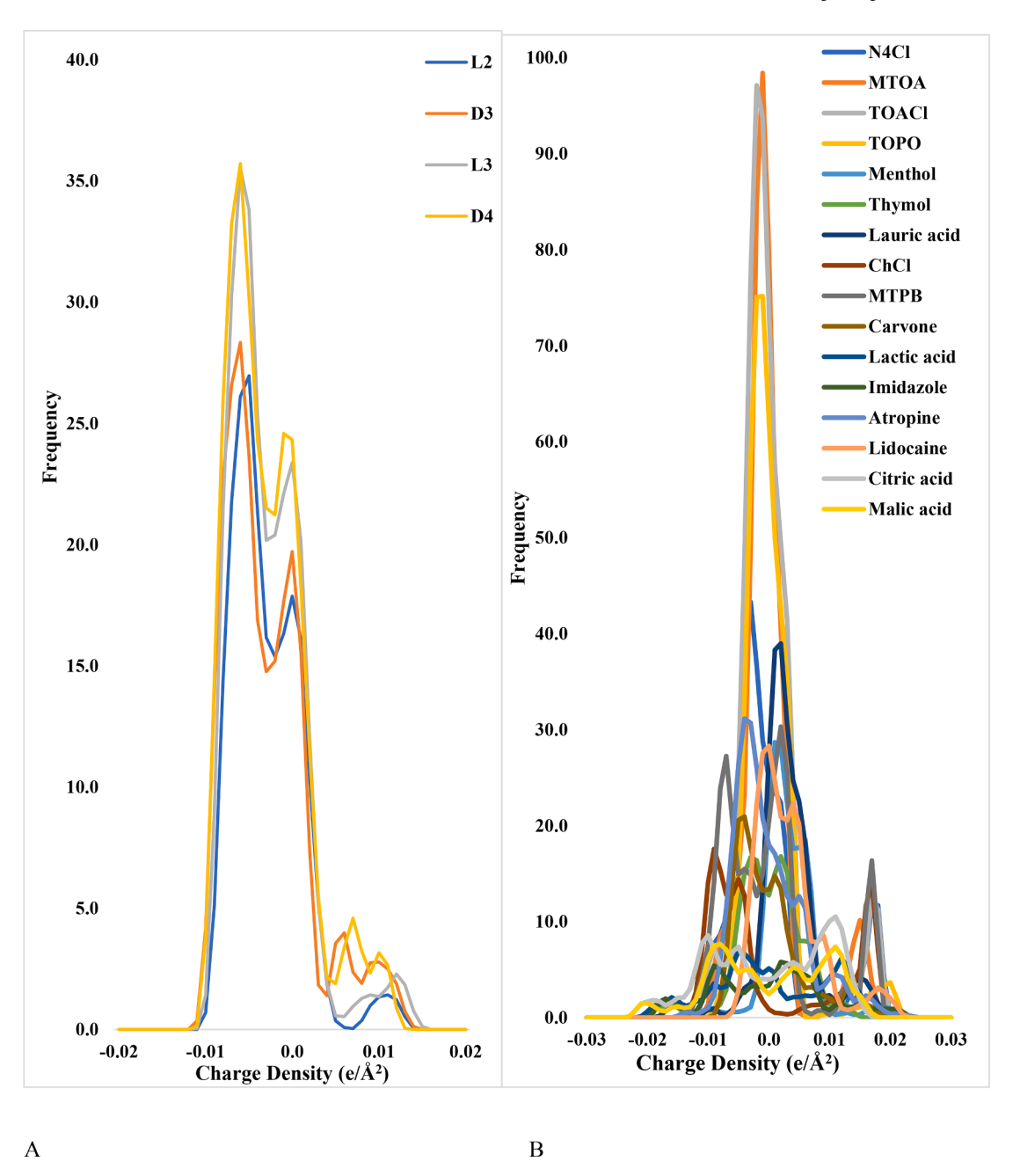


Fig. 2. (A) Sigma profiles of siloxanes as computed by TmoleX19 at B3LYP, BP-DEF2-TZVP level. (B) Sigma profiles of HBA DES components. This is how the solvent environment will look. The red line crosses the x-axis at the corresponding charge of Fig. 4 for comparison of selective capabilities for each DES component.

between DES and siloxane compounds, ionic interactions were omitted from the discussion. Negative sigma values outside of the Vander Waals region indicate hydrogen bond donating regions and positive sigma values higher than 0.079 e/Ų are representing hydrogen bond accepting regions. These histograms further support the conclusion that significant surface area of all siloxane compounds devoted to neutral charges resulting in Vander Waals interaction sites. Another note is the significantly less surface area the hexamethyl siloxanes L2 and D3 (162.38 and 222.46 g/gmol, respectively) are compared to the octamethyl siloxanes L3 and D4 (236.53 and 296.61 g/gmol, respectively). Table S2 contains the area distributions of these curves and shows more neutral surface area for the linear siloxanes L2 and L3 (94% and 93% respectively) than the two cyclic siloxanes D3 and D4 (88% and 91% respectively).

Fig. 3 shows the sigma potentials of the siloxane compounds. Sigma profiles are visual representations of how each chemical will behave (y-

axis) in the presence of a specifically charged surface (x-axis). As the yaxis is the predicted change in chemical potential from resting state to presence in the associated charged environment. The positive potentials indicate non-spontaneous interactions and vice versa. All of the siloxane compounds in this Fig. 3 are hydrophobic as indicated by the curve behavior around x = 0 as the y-values are all negative, implying an affinity towards non-polar surfaces. This observation coincides with literature as siloxane compounds can be used to impart hydrophobic properties [66,67]. These siloxane compounds are all repulsed by charge dense regions to similar degrees as the potentials for the curves at > 0.0078 e/Å^2 are all positive. The main difference is evident near the charge deficient environments ($< -0.0078 \text{ e/Å}^2$) where the siloxane compound curves exhibit a mix of attractive and repulsive interactions. At strongly charge deficient regions (< -0.015 e/Å²) the siloxane compounds are either strongly attracted (L2, L3, D3) or neutral (D4). However, as seen by Fig. 2B the HBA of the DES contain little if any

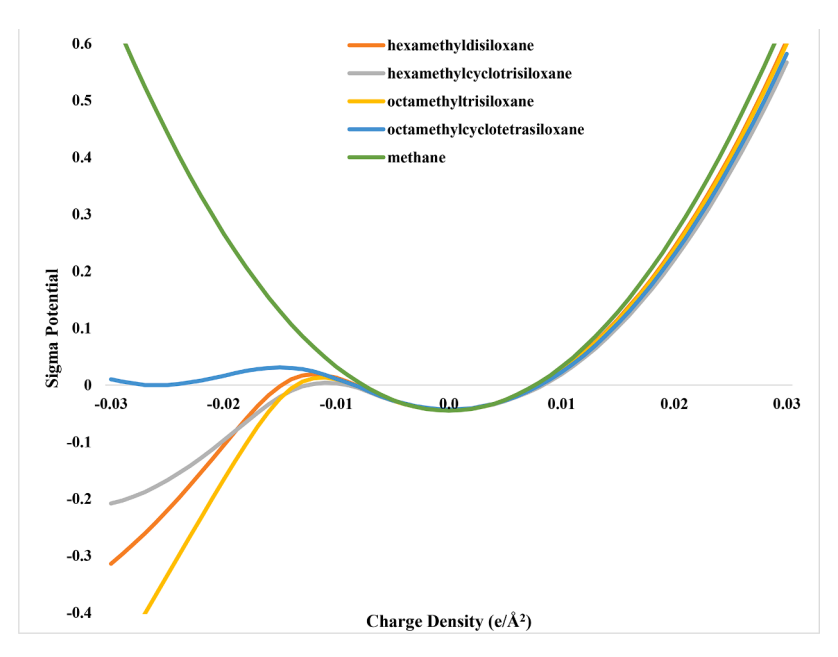


Fig. 3. Solute potentials for siloxanes and methane. The x-axis is the charge of the conductor surface, y-axis is the chemical potential of the analyte for interacting with the charged conductor surface. The separations will occur in the HB donating region due to the overlapping of most solutes and methane. By tuning a solvent with respect to its HB donating ability one can selectively absorb one solute over another.

surface charges in this region, making the relevant hydrogen bond donating zones limited to $-0.015 \, \mathrm{e/\mathring{A}^2} > x > -0.0078 \, \mathrm{e/\mathring{A}^2}$. This region exhibits an order for the siloxane compounds from least to most repulsed of D3, L3, L2, D4. The order could be due to the complex surface area charge distributions and structuring. This region is indeed significant as any separations would be dependent upon it due to the uniformity of the other two regions. When considering suitable DES, the attribute of charge deficient regions will determine the degree of selectivity found between siloxane compounds and any product, whereas the presence of Vander Waals interaction sites and absence of charge dense regions will likely play a considerable role in total solubility for siloxane compounds.

3.3. Absorption of siloxane compounds on DES

The DES were measured by their solvating capability for the four siloxane compounds through thermodynamic properties, namely activity coefficients. Activity coefficients can be used in such predictive screening procedures as they are computationally inexpensive and robust indicators of relative solubility [68–70]. Direct correlations have been made for COSMO-RS derived infinite dilution ln activity coefficients and solubility of similar complex multi-component systems. One such correlation was recently made by Mood et al. [71], where several predicted properties were analyzed for correlation with lignin solubility in ionic liquids, where Infinite dilution ln activity coefficients proved the most reliable predictors. A similar tactic is used by Mohan et al. [68] in multiple works where the ln activity at infinite dilution is used to predict plastic solubility and/or conversions. The activity coefficients were calculated for each siloxane compound with respect to each DES at infinite dilution and reported in table S1. Solvents 152-156 (MEA, DEA, MDEA, DPEG blend, and methanol) are conventional solvents which were included as a benchmarking for the prospective DES. Fig. 4 is comprised of 3 parts (a, b, and c) which represents the calculated In activity coefficients for each siloxane in the 150 solvents broken into increments of 50 solvents per sub-figure. The first 50 solvents in Fig. 4a are all above 1 and many in Fig. 4b and c. Values of $ln\gamma=1$ indicate the interactions between the DES and siloxane compounds produce no significant deviations from ideal solubilization determined through Raoult's Law. Values of $ln\gamma > +1$ indicate positive deviation or repulsive non-ideal effects, and $ln\gamma < +1$ for attractive effects. Thus,

anything above 1 is considered ineligible for the application due to sufficiently repulsive interactions.

Solvents 6-23, and 57-98 are well above the cutoff of 1. This range includes all the type 3 DES (tetrabutylammonium bromide, atropine, choline chloride, methyltriphenyl phosphonium bromide, malic acid, and citric acid based solvents) and four of the five conventional solvents (DEA, MEA, MDEA, and methanol), leaving only type 5 DES as potential candidates for siloxane compound absorptions. The reason for bias towards type 5 DES is likely due to what was presented in Section 3.2 about the repulsive effects of non-neutral charged surfaces for the siloxane compounds as hydrophobicity for a solvent requires a significant weight in the volume of Vander Waals interaction sites. Of the represented type 5 DES, terpene and tetraoctyl-based solvents are consistently showing the lowest lny for the siloxanes whereas the shorter alkyl chain lengths (95-113) show less affinity. Moreover, thymol-based solvents stand out as the most affine for siloxane compounds. As for the difference in interaction potential witnessed between the type 5 DES it is likely attributed to the degree and distribution of the components regarding surface charged area available for proton donation and acceptance.

Siloxane D3 is shown to be best solvated by DES 144 (thymol: stearic acid, 4:1) as it consistently holds the lowest activity coefficient in any given solvent as available in table S2. Through a comparison of this observation and table S2, it is apparent that siloxane D3 has the most charge dense interaction sites available of the four siloxane compounds. This coupled with thymol containing the most charge deficient area distribution (Fig. 2B, table S2), and the composition of the solvent as having four moles of thymol make a strong argument for the reason behind this result being due to the complimentary charge distributions. It is evident that the siloxane D3 is more readily solubilized in the studied DES than the others, followed by L3. This observation is likely explained through the evidence in Fig. 3 which shows these siloxane compounds are the least repulsed by hydrogen bond donors present in DES. This is further confirmed through a Pearson correlation matrix (table S3 value of -0.98 between ln activity coefficients of siloxane compounds in DES and the hydrogen bond accepting ability of the siloxane compounds. Furthermore, the work of Helstowska et al. shows of the 90 solvent combinations studied, acid based HBD's produced the highest affinity for siloxane compounds [38].

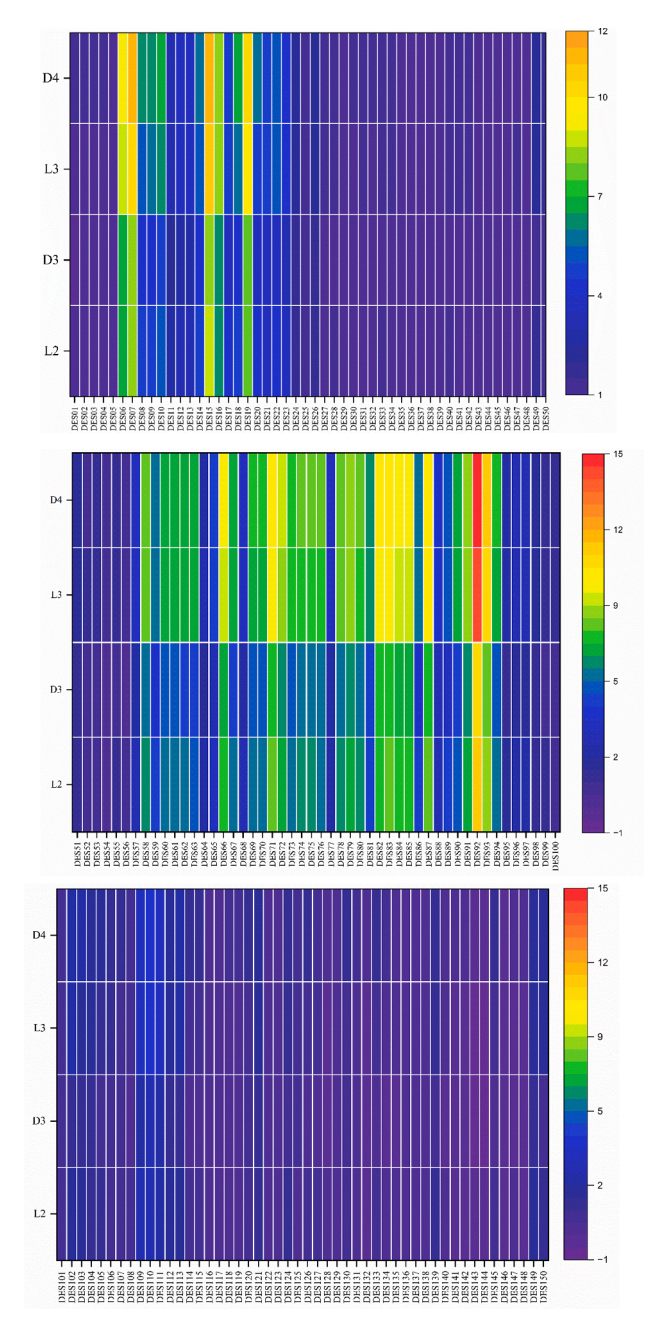


Fig. 4. In gamma values for siloxanes in 150 DES. The color legend represents In activity values broken into increments of 50 solvents per figure. Each solvent is identified by its numbering and can be matched to the supplementary table S1 for exact values and compositions. Figs. 4b and 4c contain some solvents with In activity coefficients between 1 and -1. Values in this range indicate solvent-solute affinity and therefore light to strong solubilization power. This figure represents the first phase of screening.

3.4. Excess enthalpy of extraction of siloxane compounds in DES

Table 2 contains excess enthalpy values for the thymol-based solvents due to their superior performance as outlined in Section 3.3. The solvent number is paired with each siloxane compound in the table. The enthalpy of mixing associated with hydrogen bonding (H_{HB}), Vander Waals (H_{vdw}) interactions, misfit factor (H_{mf}), and total enthalpic gain/release (+/- respectively) (H_{int}) is reported in the Table 2 as calculated through COSMOthermX. Negative values correspond to favorable interactions as the resulting energetic state of the siloxane compound in DES is lower than the siloxane compound in pure form.

Table 2 Enthalpy of mixing values for siloxanes L2, L3, D3, and D4 in thymol-based DES represented by solvent numbers. H_{int} is the total enthalpic gain (+) or loss (-) due to mixing. All values are expressed as kcal/mol. H_{MF} is the enthalpic mixing contribution from the misfitting of charges and geometry, H_{HB} is the hydrogen bonding contribution to enthalpy of mixing, and H_{vdw} is the Vander Waals contribution to enthalpy of mixing.

Solvent	Siloxane	H _{int} (kcal/ mol)	H _{MF} (kcal/ mol)	H _{HB} (kcal/ mol)	H _{vdW} (kcal/ mol)
140	L2	-6.49	1.8	-0.5	-10.99
140	D3	-7.54	2.5	-0.7	-12.47
140	L3	-8.22	2.41	-0.87	-14.34
140	D4	-9.31	2.82	-0.33	-15.77
141	L2	-7.26	1.63	-1.15	-10.93
141	D3	-8.72	2.28	-1.7	-12.44
141	L3	-9.6	2.19	-1.94	-14.37
141	D4	-10.1	2.61	-0.96	-15.72
142	L2	-7.36	1.49	-1.08	-10.97
142	D3	-8.75	2.16	-1.58	-12.46
142	L3	-9.67	2.01	-1.82	-14.39
142	D4	-10.22	2.43	-0.86	-15.76
143	L2	-7.41	1.57	-1.22	-10.96
143	D3	-8.95	2.22	-1.82	-12.48
143	L3	-9.85	2.12	-2.06	-14.42
143	D4	-10.33	2.54	-1.05	-15.78
144	L2	-7.45	1.6	-1.29	-10.96
144	D3	-9.06	2.23	-1.93	-12.49
144	L3	-9.95	2.15	-2.18	-14.44
144	D4	-10.4	2.57	-1.15	-15.79
147	L2	-6.72	1.64	-0.55	-11.02
147	D3	-7.81	2.33	-0.77	-12.5
147	L3	-8.56	2.21	-0.96	-14.38
147	D4	-9.59	2.61	-0.36	-15.81
148	L2	-7.18	1.5	-0.86	-11.02
148	D3	-8.57	2.13	-1.31	-12.53
148	L3	-9.33	2.02	-1.46	-14.44
148	D4	-10.19	2.42	-0.74	-15.84
149	L2	-5.65	2.28	-0.16	-10.99
149	D3	-6.69	2.89	-0.25	-12.46
149	L3	-6.97	3.02	-0.27	-14.3
149	D4	-8.53	3.4	-0.15	-15.75
151	L2	-7.46	1.53	-1.22	-10.97
151	D3	-8.99	2.18	-1.81	-12.5
151	L3	-9.91	2.07	-2.06	-14.44
151	D4	-10.39	2.48	-1.04	-15.8

All thymol-based type 5 DES reported in Table 2 have negative Hint which is expected as they were deemed highly favorable for solubilizing siloxane compounds in Section 3.3. Furthermore, the degree of negativity follows that of the lny negativity results where solvent 144 (thymol: stearic acid, 4:1) and solvent 151 (thymol: hexadecanoic acid, 2:1) are determined to be the most affine for the siloxane compounds and solvent 149 (thymol: betaine, 3:1) is the least. While there is an agreement between general results between the two terms of lny and H_{int} , there is a discrepancy regarding the ordering of the siloxane compounds themselves. For lny, it was seen that the ordering from most-toleast negative values were consistently ranked as D3 > L3 > L2 > D4. The general ranking for H_{int} is in reverse trend. The likely reason for the discrepancy is the accounting for Vander Waals interactions in Hint denoted as H_{vdw} and the reliance of hydrogen bonding for lny. Clearly from Table 2 the Vander Waals are significantly more impactful than the hydrogen bonds formed from siloxane-DES interactions by an order of magnitude. For instance, solvent 144 (thymol: stearic acid, 4:1) for siloxane D4 has H_{vdw} of -15.8 compared to H_{HB} of -1.15 kJ/mol. This observation is in line with the discussion from Section 3.2, as there is significantly more neutrally charged surface than is present for hydrogen bonding in both the DES and all four siloxane compounds. Also as predicted from Section 3.2, the positive values for H_{mf} overshadow the enthalpic release generated by H_{HB} as the methyl groups make reaching the negatively charged oxygen surfaces difficult. On this note the cyclical siloxanes have higher H_{mf} values as compared to linear

Table 3

Environmental Health and Safety (EHS) report for all studied DES and conventional solvents for comparison. Values predicted by VEGA software. Green indicates absence of the associated attribute, Red indicates presence of the property, and blue means indeterminate as there exists conflicting predictions, experimental values, and/or unreliable accuracy.

DES	Componen t	Persisten ce Air	Persisten ce Water	Persisten ce Soil	Mutagenici ty	Toxicit y	BCF	Carcinogenic ity
140	Camphor	b	g	g	g	g	g	g
141	Capric acid	g	g	g	g	r	g	g
142	Lauric acid	g	b	g	g	r	g	b
143	Myristic acid	g	g	g	g	g	g	g
144	Stearic acid	g	g	g	g	g	g	g
147	Undecenoic acid	g	g	g	g	g	b	g
148	Borneol	g	g	g	g	g	g	g
149	Betaine	b	b	b	g	g	b	b
151 140-	Hexadecan oic acid	g	g	g	g	r	g	g
151	Thymol	g	g	g	g	r	g	g

but are significantly more exothermic due to H_{vdw} interactions occurring on larger surface areas attributed to the size of the cyclical vs linear compounds.

3.5. Toxicology assessment of DES suitable for siloxane compounds

Type 3 DES have been heralded for their nontoxic and environmentally benign properties. However, the DES studied include a significant amount of type 5 DES. Consequently, an EHS has been conducted on the thymol-based solvents to assess them for sustainability. Thymol-based type 5 DES were chosen for VEGA EHS study due to their superior results as discussed in Section 3.3. Table 3 contains the results of the EHS study. The columns are marked as EHS property and the rows as the DES components in pure form. EHS data is unavailable for DES compounds, therefore, individual HBA and HBD are selected for EHS study. The color scheme indicates whether a result is determined to contain the respective attribute and the confidence of the output from VEGA. Green indicates that the models generally agree that the concerning property is not associated with the chemical. Blue represents inconsistent predictions for which no determination could be made. Red is given to properties that have concerning properties attributed to the chemical. For a chemical to be attributed it must have at least a moderate risk associated with it regarding the property based upon conventional determination methods (NFPA > 2 or OSCH < 3). The results of the EHS study were checked for consistency through literature by means of safety data sheets from Fischer Scientific [72] for available properties and is found that all components are considerably safe alternatives to conventional solvents [152-156]. The main discrepancies found between literature and VEGA model software predictions are for the toxicity models, for which the four predicted toxic substances of thymol, lauric, capric and hexadecenoic acids were found to be nontoxic in literature (toxicity category of 3 or 4). For example, while considered corrosive thymol is reported as nontoxic, contrary to the results from the VEGA model as it contains an acute NFPA oral toxicity factor of 4 [73]. Therefore, all components are deemed nontoxic in the list of thymol based DES components presented.

4. Conclusions

Type 3 and type 5 DES were analyzed for their potential to absorb siloxane compounds. Through sigma surface, sigma profiles, and sigma potentials of a total of 151 known DES, it was determined type 5 DES outperformed the type 3 solvents due to the steric hindrance of the

hydrogen bond accepting sites of the siloxane compounds by the methyl groups they contain. With the information gained from activity coefficient and excess enthalpy of mixing, the discrepancy between literature as whether hydrogen bonding or Vander Waals interactions dominate in solubilizing siloxane compounds is answered as being Vander Waals with an enthalpic release of an order of magnitude higher than the hydrogen bonds. A performed EHS study concludes the high performing thymol-based DES as environmentally sustainable due to low toxicity, negligible persistence (in soil, water, and air), non-mutagenic properties, negligible BCF concerns, and non-carcinogenic attributes. These insights are presented to the scientific community as evidence that DES are suitable solvents for consideration in siloxane compounds.

Funding information

This work was funded through the Petroleum Research Fund by the American Chemical Society (PRF # 60342-DNI9) and by the National Science Foundation under Grant No. 2123495.

Declaration of Competing Interest

The authors declare that they have no known competing financial interests or personal relationships that could have appeared to influence the work reported in this paper.

Data availability

Data will be made available on request.

Acknowledgements

This work was funded through the Petroleum Research Fund by the American Chemical Society (PRF # 60342-DNI9) and by the National Science Foundation under Grant No. 2123495.

Supplementary materials

Supplementary material associated with this article can be found, in the online version, at doi:10.1016/j.ceja.2023.100489.

References

- "Treatment of siloxanes in biogas: origin, effect and management," Condorchem Envitech, Aug. 09, 2018. https://condorchem.com/en/blog/siloxanes-biogas-treat ment/(accessed Aug. 03, 2022).
- [2] E.Y. Companioni-Damas, F.J. Santos, M.T. Galceran, Linear and cyclic methylsiloxanes in air by concurrent solvent recondensation-large volume injection-gas chromatography-mass spectrometry, Talanta 118 (2014) 245–252, https://doi.org/10.1016/j.talanta.2013.10.020. Jan.
- [3] J. Läntelä, S. Rasi, J. Lehtinen, J. Rintala, Landfill gas upgrading with pilot-scale water scrubber: performance assessment with absorption water recycling, Appl. Energy 92 (2012) 307–314, https://doi.org/10.1016/j.apenergy.2011.10.011. Apr.
- [4] M. Shen, Y. Zhang, D. Hu, J. Fan, G. Zeng, A review on removal of siloxanes from biogas: with a special focus on volatile methylsiloxanes, Environ. Sci. Pollut. Res. 25 (31) (2018) 30847–30862. https://doi.org/10.1007/s11356-018-3000-4. Nov.
- [5] A.A. Bletsou, A.G. Asimakopoulos, A.S. Stasinakis, N.S. Thomaidis, K. Kannan, Mass loading and fate of linear and cyclic siloxanes in a wastewater treatment plant in Greece, Environ. Sci. Technol. 47 (4) (2013) 1824–1832, https://doi.org/ 10.1021/es304369b, Feb.
- [6] T. Matsui, S. Imamura, Removal of siloxane from digestion gas of sewage sludge, Bioresour. Technol. 101 (1, Supplement) (2010) S29–S32, https://doi.org/ 10.1016/j.biortech.2009.05.037. Jan.
- [7] M. Ajhar, M. Travesset, S. Yüce, T. Melin, Siloxane removal from landfill and digester gas – a technology overview, Bioresour. Technol. 101 (9) (2010) 2913–2923, https://doi.org/10.1016/j.biortech.2009.12.018. May.
- [8] N. de Arespacochaga, J. Raich-Montiu, M. Crest, J.L. Cortina, Presence of siloxanes in sewage biogas and their impact on its energetic valorization, in: V. Homem, N. Ratola (Eds.), Volatile Methylsiloxanes in the Environment, Springer International Publishing, Cham, 2020, pp. 131–157, https://doi.org/10.1007/698_ 2018 372.
- [9] "Federal register, Volume 61 Issue 23 (Friday, February 2, 1996)." https://www.govinfo.gov/content/pkg/FR-1996-02-02/html/96-1721.htm (accessed Aug. 21, 2022).
- [10] A. Cabrera-Codony, M.A. Montes-Morán, M. Sánchez-Polo, M.J. Martín, R. Gonzalez-Olmos, Biogas upgrading: optimal activated carbon properties for siloxane removal, Environ. Sci. Technol. 48 (12) (2014) 7187–7195, https://doi. org/10.1021/es501274a, Jun.
- [11] S. Genualdi, et al., Global distribution of linear and cyclic volatile methyl siloxanes in air, Environ. Sci. Technol. 45 (8) (2011) 3349–3354, https://doi.org/10.1021/ es200301i. Apr.
- [12] S. Manahan, Environmental Chemistry, 10th ed., CRC Press, Boca Raton, 2017 https://doi.org/10.1201/9781315160474.
- [13] G.L. Daly, F. Wania, Organic contaminants in mountains, Environ. Sci. Technol. 39 (2) (2005) 385–398, https://doi.org/10.1021/es048859u. Jan.
- [14] A.L. Quinn, et al., In vitro and in vivo evaluation of the estrogenic, androgenic, and progestagenic potential of two cyclic siloxanes, Toxicol. Sci. 96 (1) (2007) 145–153, https://doi.org/10.1093/toxsci/kfl185. Mar.
- [15] A.L. Quinn, et al., Effects of octamethylcyclotetrasiloxane (D4) on the luteinizing hormone (LH) surge and levels of various reproductive hormones in female Sprague–Dawley rats, Reprod. Toxicol. 23 (4) (2007) 532–540, https://doi.org/ 10.1016/j.reprotox.2007.02.005. Jun.
- [16] J.M. McKim Jr., P.C. Wilga, W.J. Breslin, K.P. Plotzke, R.H. Gallavan, R.G. Meeks, Potential estrogenic and antiestrogenic activity of the cyclic siloxane octamethylcyclotetrasiloxane (D4) and the linear siloxane hexamethyldisiloxane (HMDS) in immature rats using the uterotrophic assay, Toxicol. Sci. 63 (1) (2001) 37–46, https://doi.org/10.1093/toxsci/63.1.37. Sep.
- [17] B. He, et al., Octamethylcyclotetrasiloxane exhibits estrogenic activity in mice via ERα, Toxicol. Appl. Pharmacol. 192 (3) (2003) 254–261, https://doi.org/10.1016/ S0041-008X(03)00282-5. Nov.
- [18] F. Accettola, G.M. Guebitz, R. Schoeftner, Siloxane removal from biogas by biofiltration: biodegradation studies, Clean Technol. Environ. Policy 10 (2) (2008) 211–218, https://doi.org/10.1007/s10098-007-0141-4. May.
- [19] M.E. López, E.R. Rene, M.C. Veiga, C. Kennes, Biogas technologies and cleaning techniques, in: E. Lichtfouse, J. Schwarzbauer, D. Robert (Eds.), Environmental Chemistry for a Sustainable World: Volume 2: Remediation of Air and Water Pollution, Springer Netherlands, Dordrecht, 2012, pp. 347–377, https://doi.org/ 10.1007/978-94-007-2439-6-9.
- [20] R. Noorain, T. Kindaichi, N. Ozaki, Y. Aoi, A. Ohashi, Biogas purification performance of new water scrubber packed with sponge carriers, J. Clean. Prod. 214 (2019) 103–111, https://doi.org/10.1016/j.jclepro.2018.12.209. Mar.
- [21] K. Starr, X. Gabarrell, G. Villalba, L. Talens, L. Lombardi, Life cycle assessment of biogas upgrading technologies, Waste Manag. 32 (5) (2012) 991–999, https://doi. org/10.1016/j.wasman.2011.12.016. May.
- [22] J. Niesner, D. Jecha, P. Stehlik, Biogas upgrading techniques: state of art review in European region, Chem. Eng. Trans. 35 (2013) 517–522, https://doi.org/10.3303/ CET1335086. Sep.
- [23] M. Struk, I. Kushkevych, M. Vítězová, Biogas upgrading methods: recent advancements and emerging technologies, Rev. Environ. Sci. Biotechnol. 19 (3) (2020) 651–671, https://doi.org/10.1007/s11157-020-09539-9. Sep.
- [24] A.I. Adnan, M.Y. Ong, S. Nomanbhay, K.W. Chew, P.L. Show, Technologies for biogas upgrading to biomethane: a review, Bioengineering 6 (4) (2019), https:// doi.org/10.3390/bioengineering6040092. Art. no. 4, Dec.
- [25] L. Zhu, G.W. Schade, C.J. Nielsen, Real-time monitoring of emissions from monoethanolamine-based industrial scale carbon capture facilities, Environ. Sci. Technol. 47 (24) (2013) 14306–14314, https://doi.org/10.1021/es4035045. Dec.

- [26] L. Brickett, Carbon Dioxide Capture Handbook, U.S. Department of Energy, 2015. Aug. [Online]. Available: chrome-extension://efaidnbmnnnibpcajpcglclefindmkaj/, https://www.netl.doe.gov/sites/default/files/netl-file/Carbon-Dioxide-Capture-Handbook-2015.pdf.
- [27] Merched Azzi, Dennys Angove, Narendra Dave, Stuart Day, Thong Do, Paul Feron, Sunil Sharma, Moetaz Attalla, Mohammad Abu Zahra, Emissions to the atmosphere from amine-based post combustion CO2 capture plant– regulatory aspects, OGST J. (2014)
- [28] A. Carranza-Abaid, R.R. Wanderley, H.K. Knuutila, J.P. Jakobsen, Analysis and selection of optimal solvent-based technologies for biogas upgrading, Fuel 303 (2021), 121327, https://doi.org/10.1016/j.fuel.2021.121327. Nov.
- [29] R. Sadegh-Vaziri, M. Amovic, R. Ljunggren, K. Engvall, A medium-scale 50 MW fuel biomass gasification based bio-SNG plant: a developed gas cleaning process, Energies 8 (6) (2015), https://doi.org/10.3390/en8065287. Art. no. 6, Jun.
- [30] T. Quaid, M.T. Reza, Carbon capture from biogas by deep eutectic solvents: a COSMO study to evaluate the effect of impurities on solubility and selectivity, Clean Technol. 3 (2) (2021), https://doi.org/10.3390/cleantechnol3020029. Art. no. 2, Jun.
- [31] A.P. Abbott, G. Capper, D.L. Davies, R.K. Rasheed, V. Tambyrajah, Novel solvent properties of choline chloride/urea mixtures, Chem. Commun. (1) (2003) 70–71, https://doi.org/10.1039/B210714G. Jan.
- [32] M.A.R. Martins, S.P. Pinho, J.A.P. Coutinho, Insights into the nature of eutectic and deep eutectic mixtures, J. Solut. Chem. 48 (7) (2019) 962–982, https://doi.org/ 10.1007/s10953-018-0793-1. Jul.
- [33] "SciELO Brazil use of natural deep eutectic solvents for polymerization and polymer reactions use of natural deep eutectic solvents for polymerization and polymer reactions." https://www.scielo.br/j/jbchs/a/fSYnzjCc6Tg5b5KvY3F7 NMJ/?lang=en (accessed Aug. 08, 2022).
- [34] D.J.G.P. van Osch, C.H.J.T. Dietz, S.E.E. Warrag, M.C. Kroon, The curious case of hydrophobic deep eutectic solvents: a story on the discovery, design, and applications, ACS Sustain. Chem. Eng. 8 (29) (2020) 10591–10612, https://doi. org/10.1021/acssuschemeng.0c00559. Jul.
- [35] H. Ren, S. Lian, X. Wang, Y. Zhang, E. Duan, Exploiting the hydrophilic role of natural deep eutectic solvents for greening CO2 capture, J. Clean. Prod. 193 (2018) 802–810, https://doi.org/10.1016/j.jclepro.2018.05.051. Aug.
- [36] Y. Bi, Z. Hu, X. Lin, N. Ahmad, J. Xu, X. Xu, Efficient CO2 capture by a novel deep eutectic solvent through facile, one-pot synthesis with low energy consumption and feasible regeneration, Sci. Total Environ. 705 (2020), 135798, https://doi.org/ 10.1016/j.scitotenv.2019.135798. Feb.
- [37] E. Stupek, P. Makoś-Chelstowska, J. Gębicki, Removal of siloxanes from model biogas by means of deep eutectic solvents in absorption process, Materials (Basel) 14 (2) (2021), https://doi.org/10.3390/ma14020241. Jan.
- [38] P. Makoś-Chelstowska, E. Słupek, A. Kramarz, J. Gębicki, New carvone-based deep eutectic solvents for siloxanes capture from biogas, Int. J. Mol. Sci. 22 (17) (2021), https://doi.org/10.3390/ijms22179551, Art. no. 17. Jan.
- [39] P. Villarim, E. Genty, J. Zemmouri, S. Fourmentin, Deep eutectic solvents and conventional solvents as VOC absorbents for biogas upgrading: a comparative study, Chem. Eng. J. 446 (2022), 136875, https://doi.org/10.1016/j. cei.2022.136875. Oct.
- [40] A. Klamt, Conductor-like screening model for real solvents: a new approach to the quantitative calculation of solvation phenomena, J. Phys. Chem. 99 (7) (1995) 2224–2235, https://doi.org/10.1021/j100007a062. Feb.
- [41] Z. Song, et al., Systematic screening of deep eutectic solvents as sustainable separation media exemplified by the CO2 capture process, ACS Sustain. Chem. Eng. 8 (23) (2020) 8741–8751, https://doi.org/10.1021/acssuschemeng.0c02490. Jun.
- [42] H. Qin, Z. Song, H. Cheng, L. Deng, Z. Qi, Physical absorption of carbon dioxide in imidazole-PTSA based deep eutectic solvents, J. Mol. Liq. 326 (2021), 115292, https://doi.org/10.1016/j.molliq.2021.115292. Mar.
- [43] Y. Zhang, X. Ji, X. Lu, Choline-based deep eutectic solvents for CO2 separation: review and thermodynamic analysis, Renew. Sustain. Energy Rev. 97 (2018) 436–455, https://doi.org/10.1016/j.rser.2018.08.007. Dec.
 [44] "TURBOMOLE documentation & how to," TURBOMOLE. https://www.turbomole.
- [44] "TURBOMOLE documentation & how to," TURBOMOLE. https://www.turbomole-org/turbomole/turbomole-documentation/(accessed Jun. 26, 2022).
- [45] K. Paduszyński, M. Królikowska, Interactions between molecular solutes and task-specific ionic liquid: measurements of infinite dilution activity coefficients and modeling, J. Mol. Liq. 221 (2016) 235–244, https://doi.org/10.1016/j.molliq.2016.05.063. Sep.
- [46] F. Bezold, M.E. Weinberger, M. Minceva, Assessing solute partitioning in deep eutectic solvent-based biphasic systems using the predictive thermodynamic model COSMO-RS, Fluid Phase Equilib. 437 (2017) 23–33, https://doi.org/10.1016/j. fluid.2017.01.001. Apr.
- [47] K. Wichmann, "COSMOthermX user guide," p. 131.
- [48] "BIOVIA COSMOconf, BIOVIA COSMO-RS Dassault systèmes®." https://www. 3ds.com/products-services/biovia/products/molecular-modeling-simulation/so lvation-chemistry/biovia-cosmoconf/(accessed Aug. 21, 2022).
- [49] P. Arenas, I. Suárez, B. Coto, Combination of molecular dynamics simulation, COSMO-RS, and experimental study to understand extraction of naphthenic acid, Sep. Purif. Technol. 280 (2022), 119810, https://doi.org/10.1016/j. seppur.2021.119810. Jan.
- [50] E. Zurob, et al., Design of natural deep eutectic solvents for the ultrasound-assisted extraction of hydroxytyrosol from olive leaves supported by COSMO-RS, Sep. Purif. Technol. 248 (2020), 117054, https://doi.org/10.1016/j.seppur.2020.117054.
- [51] J. Cheng, H. Qin, H. Cheng, Z. Song, Z. Qi, K. Sundmacher, Rational screening of deep eutectic solvents for the direct extraction of α -tocopherol from deodorized

- distillates, ACS Sustain. Chem. Eng. 10 (25) (2022) 8216–8227, https://doi.org/10.1021/acssuschemeng.2c01992. Jun.
- [52] K.A. Kurnia, J.A.P. Coutinho, Overview of the excess enthalpies of the binary mixtures composed of molecular solvents and ionic liquids and their modeling using COSMO-RS, Ind. Eng. Chem. Res. 52 (38) (2013) 13862–13874, https://doi. org/10.1021/ie4017682. Sep.
- [53] Y. Chu, X. He, MoDoop: an automated computational approach for COSMO-RS prediction of biopolymer solubilities in ionic liquids, ACS Omega 4 (1) (2019) 2337–2343, https://doi.org/10.1021/acsomega.8b03255. Jan.
- [54] A. Klamt, From Quantum Chemistry to Fluid Phase Thermodynamics and Drug Design. Elsevier. [Online]. Available: vbk://Nv6N2OsaRD8E81A_ v2rDwsUUDzfOeb9-Zta 8LcUe 0.
- [55] A. Klamt, F. Eckert, COSMO-RS: a novel and efficient method for the a priori prediction of thermophysical data of liquids, Fluid Phase Equilib. 172 (1) (2000) 43–72, https://doi.org/10.1016/S0378-3812(00)00357-5. Jul.
- [56] "Sigma moments COSMO-RS 2022.1 documentation." https://www.scm.com/doc/COSMO-RS/advanced_scripts/Sigma_moments.html (accessed Aug. 23, 2022)
- [57] J.G. Speight, 8 Gas cleaning processes, in: J.G. Speight (Ed.), Natural Gas (Second Edition), Gulf Professional Publishing, Boston, 2019, pp. 277–324, https://doi.org/ 10.1016/B978-0-12-809570-6.00008-4
- [58] N. Ghasem, Chapter 21 CO2 removal from natural gas, in: M.R. Rahimpour, M. Farsi, M.A. Makarem (Eds.), Advances in Carbon Capture, Woodhead Publishing, 2020, pp. 479–501, https://doi.org/10.1016/B978-0-12-819657-1.0021.9
- [59] "Selexol," netl.doe.gov. https://netl.doe.gov/research/coal/energy-systems/gasification/gasifipedia/selexol (accessed Aug. 04, 2022).
- [60] V.G. KG, "Downloads | VEGA." https://www.vega.com/en-us/downloads (accessed Aug. 04, 2022).
- [61] "An overview of the biphasic dehydration of sugars to 5-hydroxymethylfurfural and furfural: a rational selection of solvents using COSMO-RS and selecti ... - Green chemistry (RSC Publishing) DOI: 10.1039/C9GC04208C." https://pubs-rsc-org. portal.lib.fit.edu/en/content/articlehtml/2020/gc/c9gc04208c (accessed Aug. 04, 2022).
- [62] S. Linke, K. McBride, K. Sundmacher, Systematic green solvent selection for the hydroformylation of long-chain alkenes, ACS Sustain. Chem. Eng. 8 (29) (2020) 10795–10811, https://doi.org/10.1021/acssuschemeng.0c02611. Jul.

- [63] H. Hong, Advances in Computational Toxicology: Methodologies and Applications in Regulatory Science, Springer, 2019.
- [64] F. Olea, et al., Separation of vanillin by perstraction using hydrophobic ionic liquids as extractant phase: analysis of mass transfer and screening of ILs via COSMO-RS, Sep. Purif. Technol. 274 (2021), 119008, https://doi.org/10.1016/j.seppur.2021.119008. Nov.
- [65] J.P. Wojeicchowski, C. Marques, L. Igarashi-Mafra, J.A.P. Coutinho, M.R. Mafra, Extraction of phenolic compounds from rosemary using choline chloride – based deep eutectic solvents, Sep. Purif. Technol. 258 (2021), 117975, https://doi.org/ 10.1016/j.seppur.2020.117975. Mar.
- [66] E. Cappelletto, et al., Hydrophobic siloxane paper coatings: the effect of increasing methyl substitution, J. Sol-Gel Sci. Technol. 62 (3) (2012) 441–452, https://doi. org/10.1007/s10971-012-2747-1. Jun.
- [67] B.Q.H. Nguyen, A. Shanmugasundaram, T.-F. Hou, J. Park, D.-W. Lee, Realizing the flexible and transparent highly-hydrophobic film through siloxane functionalized polyurethane-acrylate micro-pattern, Chem. Eng. J. 373 (2019) 68–77, https://doi.org/10.1016/j.cej.2019.04.197. Oct.
- [68] M. Mohan, J.D. Keasling, B.A. Simmons, S. Singh, In silico COSMO-RS predictive screening of ionic liquids for the dissolution of plastic, Green Chem. 24 (10) (2022) 4140–4152, https://doi.org/10.1039/D1GC03464B. May.
- [69] X. Liu, Y. Nie, Y. Liu, S. Zhang, A.L. Skov, Screening of ionic liquids for keratin dissolution by means of COSMO-RS and experimental verification, ACS Sustain. Chem. Eng. 6 (12) (2018) 17314–17322, https://doi.org/10.1021/ acssuschemeng.8b04830. Dec.
- [70] T. Brouwer, B. Schuur, Model performances evaluated for infinite dilution activity coefficients prediction at 298.15K, Ind. Eng. Chem. Res. 58 (20) (2019) 8903–8914, https://doi.org/10.1021/acs.iecr.9b00727. May.
- [71] "Multiscale molecular simulations for the solvation of lignin in ionic liquids | Scientific reports." https://www.nature.com/articles/s41598-022-25372-2#rightslink (accessed Feb. 24, 2023).
- [72] "SDS search." https://fse-search.fs-prod.cloudprod.fishersci.net/catalog/search/s dshome.html?countryCode=us&language=en (accessed Aug. 18, 2022).
- [73] "Thymol SDS (Safety data sheet) | Flinn scientific." https://www.flinnsci.com/sds 818-thymol/sds 818/(accessed Aug. 18, 2022).